SCIREA Journal of Electrical Engineering
ISSN: 2995-7141
http://www.scirea.org/journal/DEE
November 25, 2024
Volume 9, Issue 2, April 2024
https://doi.org/10.54647/dee470554

Ink-based fabrication of microwave passive devices: a review

Isabelle Huynen [1,*]

[1] Université catholique de Louvain (UCLouvain), ICTEAM Institute, Place du Levant 3, 1348 Louvain-la-Neuve, Belgium; e-mail : isabelle.huynen@uclouvain.be

Abstract: Since the last decade inkjet printing (IJP) has gained much interest in the electronics field, due to its ease of fabrication and low cost, since it does not require mask fabrication and can use cheap substrates like paper, adding the advantage of recyclability. In this manuscript, a review of IJP of microwave passive devices is presented. The various inks (dielectric or conductive), substrates (rigid or flexible), and printing techniques are first presented, with a focus on IJP. Next various passive devices are discussed. They include couplers, resonators, sensors, filters, antennas, and absorbers. For each category, the geometry, dimensions, and performances are discussed. Whenever possible, green aspects are addressed.

Keywords: 2D printing; inkjet; silver; gold; carbon nanotube, graphene; dielectric ink; coupler; filter; antenna; absorber; resonator; sensor; microwaves.

1. Introduction

3D printing technology is expected to revolutionize the development of components and systems, unifying materials and process engineering into a single process that could yield products unimaginable before. IJP can be considered a 2D or surface additive manufacturing technique. As for energy storage, 2D and 3D techniques have many mature applications in the (bio)medical, building, mechanical, and electrical engineering sectors. For the development of microwave and millimeter-wave devices operating in the 3 GHz–300 GHz frequency range, various topologies and functionalities can be addressed, such as resonators [1], capacitors [2], inductors [3], filters [4], couplers [5,6], antennas [7–9] waveguides [8,10], sensors [10], etc. This manuscript will consider the 2D additive ink-based technology for passive devices only [3,8,11–13]. While ink printing can also be used to synthesize active devices, such as diodes [14,15], and transistors [14,16].

It is widely recognized that 2D printing has several advantages. It uses a low-cost direct deposition fabrication technique that allows the versatile realization of patterns adapted to each desired application. This avoids using masking and sacrificial layers that complicate and slow the manufacturing process, especially for mass production. IJP is also reputed to reduce waste production.

This introduction is voluntarily short because the state-of-the-art concerning ink- printed microwave devices will be exhaustively reviewed in the various sections of the manuscript. Indeed it is organized as follows. At first, the various inks proposed for the printing of microwave devices are reviewed, as well as the printing tools Next each device/topology will be discussed.

2. Materials and Methods

This section reviews the types of inks used for 2D printing, the substrates used for printing, and the printing tools. The sustainability and green aspect is also addressed in the last subsection 2.3.

2.1. Inks for 2D printing

2.1.1. Conductive inks

The purpose of ink printing is to reproduce the metallic pattern of classical planar circuits usually obtained via etching/engraving of a metal layer or the deposition of a metallic track. The most important parameter of the ink is its conductivity. Various materials are reported in the literature to achieve conductivity: metal [17] involving gold [18], silver [4,11,19–23], that is compared to copper [24,25], carbon nanotubes (CNT) [26,27,34], carbon black [28] graphene [29–32], metal-oxide [33] or composite nanoparticles such as CNT decorated with metallic nanospheres [35]. Inks based on CNT were specifically characterized at microwave frequencies [36,37] for subsequent applications. For each configuration of ink, the challenge is to achieve good conductivity [1] of the deposited ink while facilitating the suspension of the particles in the liquid forming the ink. The ink formulation is crucial to ensure a uniform deposition and a reliable reproducible conductivity. Momeni et al. [38] propose reactive inks for printing planar microwave devices. Reactive inks allow to deposit/print materials that cannot easily be deposited inink form [39,40]. The formation of the desired formulation occurs on the layer via a reactionwith a material already present on the substrate.

Figure 1 illustrates a SEM image of a silver (Ag) film aqueous deposition and the resulting ink-printed RFID tag [17].

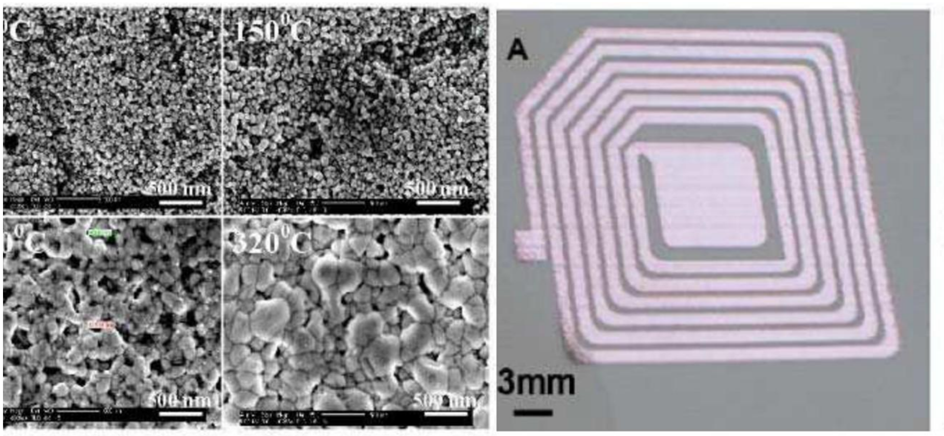

Figure 1. Left: SEM image of an Ag film aqueous deposition, for different sintering temperatures (60°, 120°, 250°, and 320°) Right: resulting printed RFID tag. Reprinted from [17] under the Creative Commons Attribution Non-Commercial License (http://creativecommons.org/licenses/ by-nc/3.0/)

Next, the level of conductivity is easily modulated by the number of printed layers. Various studies have indicated that the following relationship applies to the surface sheet resistance R_s of the deposited track, depending on the number of printed layers.

$$R_s = \frac{R}{w\,l} = \frac{1}{\sigma\, t} \qquad (1)$$

Where R is the measured resistance between the two ends of a printed strip of width w and length l, and σ and t are the conductivity and thickness of the printed strip, proportional to the number of printed layers forming the strip [34,35]. The relationship (1) is experimentally validated, according to [26], see Figure 2.

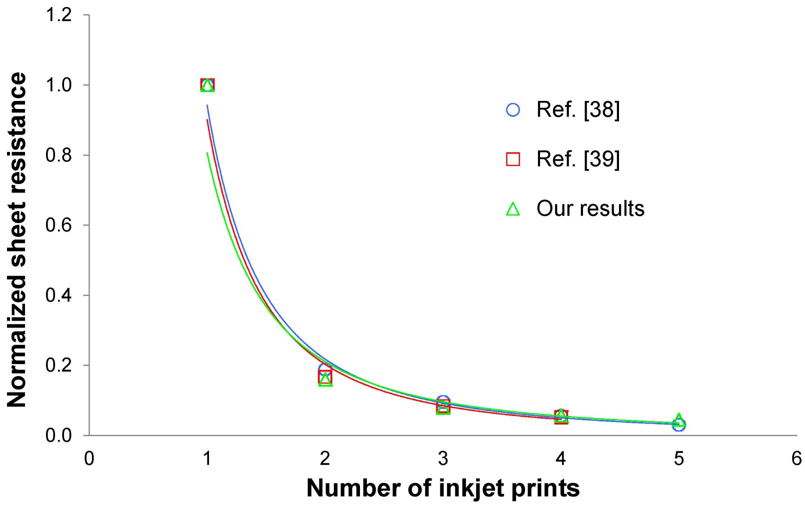

Figure 2. Normalised sheet resistance according to [26]. Reproduced under the Creative Commons Attribution Non-Commercial License by MDPI.

2.1.2. Dielectric inks

Kim et al. [10] explain that dielectric-based inks are aused for inkjet printing of substrates because they allow fabricating multilayered structures of interest for planar microwave devices. Materials considered in their study are SU-8 polymer with a UV-cross linker dissolved in cyclopentanonea for thick layers, and poly-4-vynylphenol (PVP) for thin layers.

Mohapatra et al. [42] propose to use PVP to fabricate multilayered capacitors combining inkjet-printed PVP on flexible polyimide with silver inkjet-printed electrodes.

Kim et al. [41] reported the development of barium-titanate/h-BN ink to fabricate capacitors. The dielectric constant of the $BaTiO_3$/h-BN thin films increases from 10.2 to 16 when adding 10% of $BaTiO_3$ nanoparticles to the h - BN ink.

In [43] poly(5-vinyl-2-norbornene) ink was deposited on Kapton film and copper as a low-loss dielectric substrate for printed RF and microwave devices. Measuring the dielectric loss of the poly(5-vinyl-2-norbornene) material revealed an order of magnitude improvement compared to commercially utilized printed photopolymers, the values fall within the range of commercial RF laminates, such as Rogers substrate.

In [13] Barium strontium titanate (BST) inks were used to ink-print 10 μm-thick films for the fabrication of integrated passive microwave circuits. Their dielectric properties were investigated; a dielectric constant of 240 and a loss tangent factor of 0.07 were measured at 10 GHz. As a demonstrator, a coplanar waveguide line was printed on the BST substrate as a phase shifter. It uses 18 tunable interdigital capacitors (IDCs) to apply a phase shift on a microwave signal propagating through the central waveguide. At 10 GHz a phase shift of 170 $^\circ$ and a figure of merit of 20 $^\circ$/dB was obtained.

In [44] ink writing produced bismuth molybdate ceramic substrates for wireless telecommunications applications operating at microwave frequencies, with great repeatability and properties comparable to ceramics fabricated via conventional processing routes.

Similarly, in [45] a DC-biased phase shifter is realized with BST/COC (Cyclic Olefin Copolymer) ink. A phase shift up to 49° is obtained at 12.5 GHz for a bias voltage of up to 10 V. The printed IDCs have 12 interdigitated fingers, each with a width, length, and height of 40 μm, 2000 μm, and 3 μm, respectively. The gap between IDC fingers is 40 μm.

2.2. Tools for 2D printing

The main techniques reported are spray-coating, screen printing [46], and IJP schematized in Figure 3. IJP allows the direct writing of a pattern stored digitally in the printing tool's processing unit. A review of the classification and application of IJP technology is provided in [47]. Piezoelectric IJP technology is presented as the most promising due to its reliability and ease of handling a diverse range of inks. While other technologies such as thermal IJP, electrodynamic printing, needle-based printing aerosol jet printing, laser-assisted printing, acoustic and acoustic-wave printing, or drop impact printing are also discussed. Aerosol jet printing is also proposed in [1,48]. The review in [47] also highlights the important role of viscosity since this parameter governs the quality of droplet formation and deposition on the substrate. Finally, various advantages are enumerated: the simplification of the fabrication process of devices, as IJP allows to suppress or reduce the use of masks, digital textile printing, and display pixel printing where again the maskless feature allows to speed up the fabrication process of multilayers forming the display. Large-scale production is also facilitated. The same advantages apply to MEMS device printing [49] and wireless and wearable electronics [29] or RFID tags [50–52].

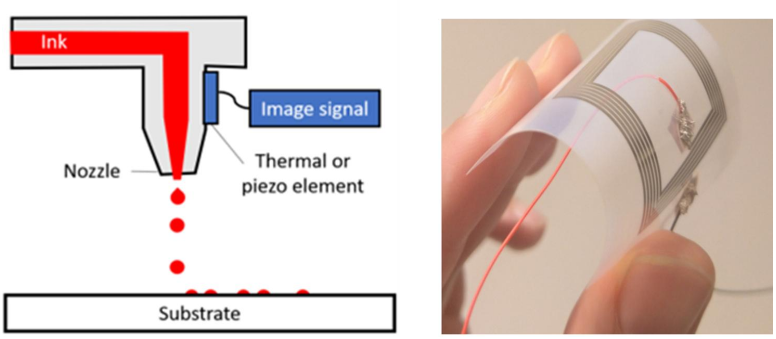

Figure 3. Left: Schematic representation of IJP process. Right: printed RFID coil. Reprinted from [62] under the terms and conditions of the Creative Commons Attribution (CC BY) license (https://creativecommons.org/licenses/by/ 4.0/).

2.3. *Sustainability and green considerations*

This section illustrates how the IJP field handles sustainability and green aspects.

Sanchez et al. [53] present a review of Sustainable Inks for Printed Electronics.

Hwang et al. [54] demonstrate the feasibility of using pollen-based materials as natural biopolymer substrates for flexible and stretchable electronics.

In [55] solutions for sustainability are discussed in the context of flexible electronics.

In [56] a green ink formulation is proposed for inkjet-printed transparent electrodes in OLEDs on biodegradable substrates.

Batet et al. [57] propose an overview of green printing electronics. Inks formulations based on carbon and silver have been chosen as conductive materials, and commercial papers and substrates based on cellulose nanofibers (CNF).

In [58] aqueous graphene inks were obtained by liquid-phase exfoliation of graphite and bonded to biodegradable polymers. Consequently, green and eco-friendly graphene inks are proposed, free of harmful organic compounds.

In [59] polymer-based conductive inks reinforced with graphene are developed based on polyvinylpyrrolidone (PVP) as polymer binder and di-hydrolevoglucosenone (Cyrene) as a solvent, leading thus to environmentally friendly conductive inks.

In [60] authors propose to use shellac - a green and sustainable material - as a multi-functional component of green, paper-based printed electronics (PE). As it is green it is used to coat paper substrates to create planarized, printable surfaces. At the end of life, shellac is used as a sacrificial layer to separate by dissolution the PE from the paper substrate.

Li et al. [61] propose a green substrate and functional inks based on bio nano-materials (nanocellulose and carbon nanoparticles) for fabricating dielectric and conductive layers using conventional inkjet technology.

Konstas et al. [50] claim a green monopole antenna fabrication. The antenna performance will be discussed in section 3.5. Here we explain only the green aspect. Authors justify it as the fact that the antenna is printed on paper, a widely available material, among the most environmentally friendly, because of its high biodegradability.

Finally, Wiklund et al. [62] address environmental aspects in their review of printed electronics. They explain that this technology has great potential to provide biodegradable and recyclable solutions allowing the reduction of the electronic waste caused by the ever-growing use of electronic devices. Among the biodegradable natural solutions for substrates, they list paper, silk, starch, and shellac, a natural resin exhibiting biodegradability, and high surface smoothness suitable for forming substrate films. For synthetic polymeric substrates, PLA, PDMS, PVA, polycaprolactone (PCL), poly-lactic-co-glycolic acid (PLGA), polyurethane (PU), polybutylene succinate (PBS) and polyethylene glycol (PEG) are examples of biodegradable polymers that can be used as substrate materials.

3. Results and discussion

This section proposes an analysis of various devices fabricated by IJP and discusses their performance and features.

3.1. Couplers

He et al. present in [5] an interdigitated Lange coupler operating around 8 GHz. The device has 6 fingers printed on a 0.51 mm thick Rogers 4003C substrate with one copper side etched off. Conductive traces were fabricated using Suntronic EMD5730 silver nanoparticle (SNP) ink; 5 layers were deposited using the Dimatix DMP 2800 Printer. A finger length 4.9 mm long and finger widths of 0.12 mm and the spacing between each as 0.09 mm, are dimensioned for a 3 dB coupling bandwidth of 5-12.5 GHz. The expected 90° phase shift is obtained experimentally at 5 GHz between the input and coupled ports. A 4 dB coupling level is observed, 1 dB lower than the specification. The authors suggest that increasing the number of printed layers would improve the coupling towards 3 dB.

In [6] a broadband coupler in Substrate Integrated Waveguide topology (SIW) is fabricated by IJP. More precisely, the top and bottom layers of the waveguide are inkjet printed on a 0.254 millimeter-thick polyimide substrate, as well as the microstrip transitions to the accesses of the SIW. The structure is printed two times, and the resulting parts are placed on the top and bottom sides of a metallic ground plane including 2 slanted slots. This topology ensures the coupling mechanism in the same way as couplers based on rigid rectangular metallic waveguides. Dimatix DMP-2800 printer is used to print silver nanoparticle ink. The authors conclude that "the proposed multilayer coupler is a first step toward the inkjet-printed multilayer electronics systems for wearable, sensing, RFID and communication systems." They also mention that the relatively high loss can be improved by printing more layers and "using low loss flexible substrates, such BCB and LCP". Indeed the direct and coupled paths show a -8 dB level of transmission instead of the nominal – 3 dB expected at 5.8 GHz.

A modified branchline 3 dB coupler is proposed in [63]. This coupler is designed to have equal power division and output phase difference of 45°. It is printed on a flexible transparent Polyethylene Terephthalate (PET) substrate using silver ink. Measurements show that a 3 dB coupling level is achieved within the frequency range of 5.09 GHz to 6.97 GHz, and a 45° phase difference is verified with a little phase variation, of about ±10 within the operational bandwidth. The total surface of the device is lower compared to similar couplers from the literature. The authors point out that "the inkjet printing technique is of low cost, readily available, and will provide a means of fast prototyping of electronic circuitries as the process does not require any thermal curing".

3.2. Capacitors

For the sake of completeness; we report here 2 works related to capacitors.

The reader should also refer to section 2.1.2 since dielectric inks are formulated for the deposition of insulating layers that are key parts of a capacitor.

In [2], an interdigital capacitor (IDC) is fabricated by deposition of conductive ink on a 127 μm-thick polyimide (Kapton) film. The authors point out that IJP is of great interest for flexible substrates in conformable and wearable devices for health monitoring. The proposed IDC has a total of 16 fingers in a parallel configuration. The fingers have been designed with a length, a width, and a spacing of 20 mm, 0.7 mm, and 0.2 mm, respectively. "The nominal IDC dimensions are 34.6 × 20.2 mm^2. Unfortunately, no experimental values of capacitance are provided.

In [64], multilayered capacitors are inkjet printed using dielectric inks. SU-8 and Poly4VinylPhenol (PVP) are used to formulate the inks, printed using a Dimatix DMP-2800 IJP platform on a flexible substrate. The Metal Insulator Metal (MIM) capacitance is realized as follows. Three layers of Cabot CCI-300 silver nanoparticle ink are printed and cured at 120 C for 1 hour in an oven to form the bottom plate with a 1.5 m thickness. The dielectric layer is then printed and cross-linked, followed by the printing and curing of three more layers of silver nanoparticle ink to form the top plate. The 1.5 x 1.5 mm^2 pad is measured and shows capacitance values of 20 and 50 pF, self-resonance frequency of 3 and 1.9 GHz for SU-8 and PVP, respectively, while they share about the same quality factor equal to 4. 2.

3.3. Resonators

Several topologies of resonators are fabricated using IJP for various applications.

A microstrip ring resonator is proposed in [65] for microfluidic applications. The substrate considered is Low-Temperature CoFired Ceramic (LTCC), stacked into 4 layers, the first supporting a ground plane, the next two ones having a semicircular engraved channel terminated by a straight feeding channel section at each end, and the last one supporting the IJP microstrip ring resonator with two coupling microstrip access lines. The inner diameter of the ring is 13.5 mm, and the outer one is 15.5 mm. The width of the microstrip line is 1 mm and the length of the feed lines was 13.4 mm. The gap between the feed lines and the ring resonator was 0.1 mm. The microstrip circuit was deposited by the Dimatix DMP-2831 ink-jet printer with ink with silver nanoparticles. The device was tested for the detection of the concentration of ethanol in water between 2.5 and 3.2 GHz. A clear shift of the resonant peak in the measured transmission is observed when the concentration increases from 10 to 90% by 20% steps. Authors conclude that IJP is a feasible technique for realizing microstrip components on LTTC substrate including microfluidic functionalities.

Paul et al. proposed microstrip square split-ring resonators for sensor applications. In [66], gold inkjet-printed split-ring resonators (SRRs) of size 18 x18 mm^2, and side-coupled to a microstrip line of length 48 mm, are proposed for detecting analytes. Again the detection is based on the observed shift of resonance in the transmission measurement. The printing process is performed with a Materials Inkjet Printer from Dimatix (DMP-2850 on a flexible 50 μm-thick Kapton substrate. The gold layer is treated to allow the grafting of bio-materials. The nominal resonant frequency is 2.65 GHz and a significant shift of – 58 MHz is observed in the presence of the analyte. The authors conclude "that since printing technologies are utilized in the industry on a roll-to-roll basis, there is potential to manufacture printed sensors for biomedical applications in large quantities at minimal cost". In [67] the same SRR structure is tested for detecting ethanol and deionized water. A shift of respectively 7.5 and 5 MHz is observed.

In [52] a microwave square resonator whose branches are formed by 4-fingers Interdigitated structures were inkjet printed on a 250 µm thick CTLE-MW laminate substrate from Rogers using silver ink and a Dimatic DMP 2800 inkjet printer. The resonator was then covered with a CNT film formed by the IJP of layers of CNT ink. This film aims to be sensitive to the presence of gas. The overall surface of the device is 10 x 10 mm^2. The detection is achieved by monitoring the change of magnitude of the transmission parameter when NH_3 is present. These results indicated that the frequency response of the microwave sensors was related to the resistance of CNT films. The shift in frequency spans from 200 to 350 MHz when NH_3 concentration varies from 300 to 700 ppm. The authors conclude that "their transmission-type microwave resonator can provide multidimensional frequency responses and high repeatability and has the potential for integration with the IoT and RFID for wireless gas-sensing applications".

In their review of microwave resonators for wearable sensor design, Royo et al. [68] show illustrations of SRRs printed on polyimide and low-cost photo paper. However, no applications for microwave and millimeter waves are discussed.

Resonators are also used as a method for measuring the dielectric properties of materials. Terhani et al. [69] proposed inkjet printing rectangular resonators on a SU-8 film. The fabricated T-resonator includes a microstrip transmission line with a length of 19.8 mm and a microstrip resonating line with a length of 19.5 mm. The authors show that the T resonator inkjet printed allows the extraction of the dielectric constant of a SU-8 substrate with a very good accuracy compared to more conventional dielectrometric methods.

3.4. Filters

Blanco et al. [4] propose a proof-of-concept of the fabrication of filters via silver IJP. The examples presented are a stepped impedance low-pass and a coupled line bandpass filter, both realized on a 1.5 mm thick low-cost FR4 type substrate. The 2 prototypes and their performance are presented in Figures 4 and 5 respectively. In both cases, the measurement agrees very well with the simulated design.

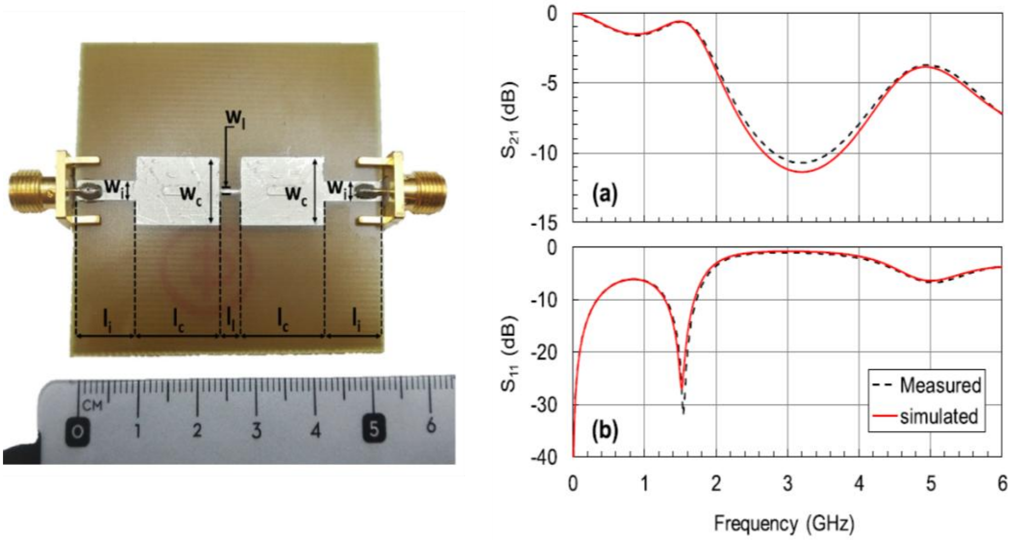

Figure 4. Stepped impedance low-pass filter having 5 sections. Left: photo and dimensions of the filter. Right: measured and simulated performance. (a) transmission (b) reflection. Reprinted from [4] under the terms and conditions of the Creative Commons Attribution (CC BY) license (https://creativecommons.org/licenses/by/ 4.0/).

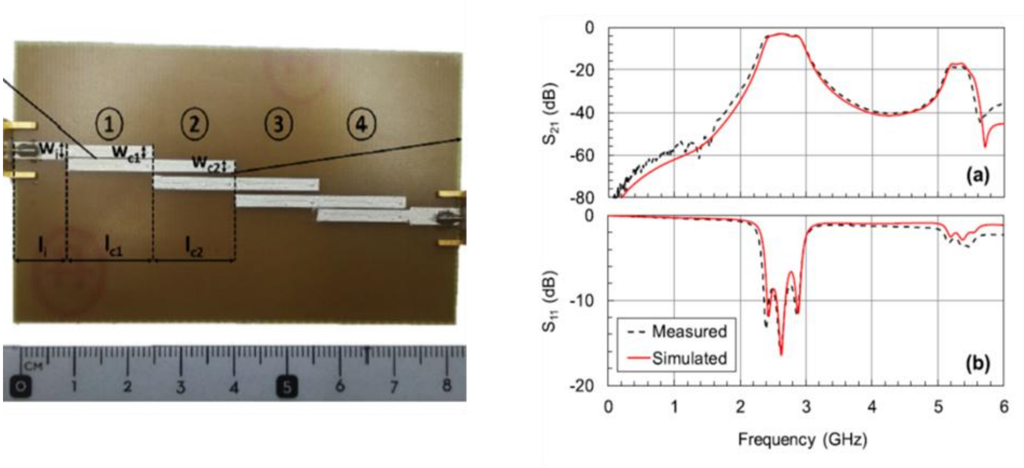

Figure 5. Left: Coupled line bandpass filter. Left: photo and dimensions of the filter containing 4 coupled sections. Right: measured and simulated performance (a) transmission (b) reflection. Reprinted from [4] under the terms and conditions of the Creative Commons Attribution (CC BY) license (https:// creativecommons.org/licenses/by/ 4.0/).

3.5. *Antennas*

Various topologies of antennas are fabricated via IJP. Some examples are discussed in this section.

In [4] a stepped-type monopole antenna with two rectangular slots added on the ground plane and two strips added to the top layer feeding line (Figure 6) resulting in bandwidth enhancement is realized on a 1.5 mm thick low-cost FR4 type substrate using silver conductive (SC) ink printing or copper deposition. The corresponding performance is presented in Figure 7. The measurement agrees very well with the simulated design. The performance is very similar for the SC and copper prototypes.

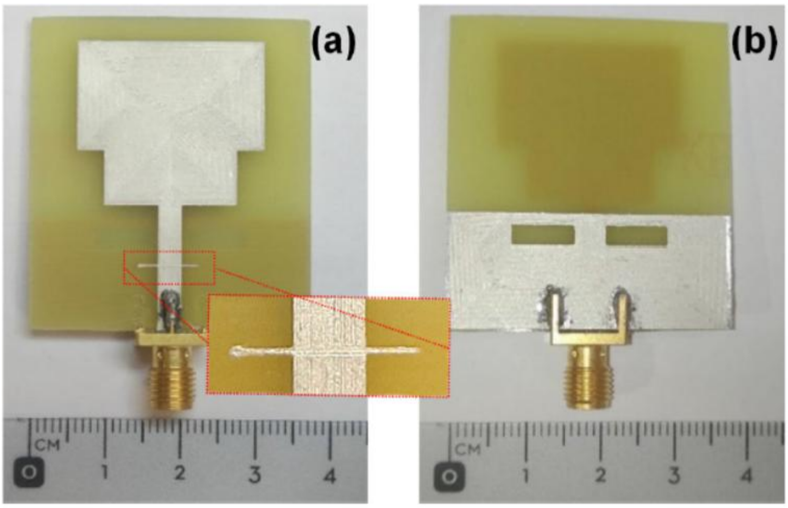

Figure 6. Stepped-type monopole antenna (a) top view (b) bottom view. Reprinted from [4] under the terms and conditions of the Creative Commons Attribution (CC BY) license (https:// creativecommons.org/licenses/by/ 4.0/).

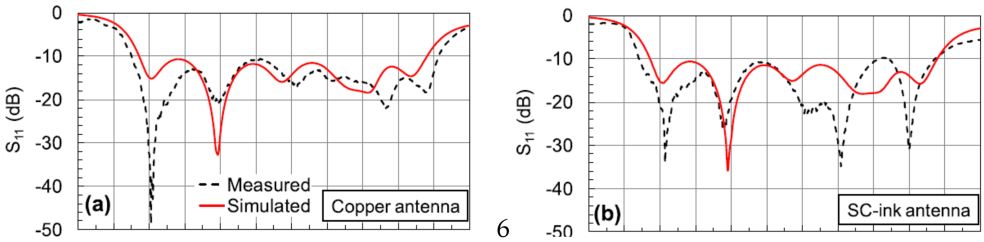

Figure 7. Simulated and measured performance of stepped-type monopole antenna (a) copper prototype (b) Silver conducting (SC) ink prototype. Reprinted from [4] under the terms and conditions of the Creative Commons Attribution (CC BY) license (https:// creativecommons.org/licenses/by/ 4.0/).

In [9] a microstrip patch antenna is proposed for operation at 2.4 GHz. A Dimatix DMP 2800 Inkjet printer (Fujifilm Dimatix, Inc. Santa Clara, USA) [is used to print the antenna geometries with nanosilver ink. The same antenna is fabricated with copper using a traditional photolithography technique for comparison. A good agreement is observed between the copper and silver ink prototypes regarding the reflection losses.

Konstas et al. [50] propose a Z-shaped monopole microstrip antenna operating at 0.9 GHz, printed on a paper substrate. The antenna structure comprises a planar Z-shaped rectangular monopole with a width of 50 mm, a length of 56 mm, and a spacing of 11 mm from the ground plane. Two rectangular slots are embedded into the radiating element from both side edges, resulting in a meander-like antenna. Silver nanoparticle ink and a Dimatic DMP 2800 inkjet printer are used. For the sake of comparison, the antenna was also fabricated with the formation of self-adhesive thin copper tape glued on the paper. The 2 prototypes have the same excellent return loss higher than 30 dB. The authors concluded that the proposed antenna on paper is interesting for answering “the need for inexpensive, reliable, and durable wireless RFID-enabled sensor nodes.”

Similarly to [52], Yang et al. [51] propose an antenna configuration for the detection of gas, based on the presence of single-wall carbon nanotubes (SWCNT). The antenna is printed on paper. Electrodes were patterned on a 100 µm-thick flexible paper substrate with nanoparticle silver ink. The electrode finger is 2 mm x 10 mm^2 with a gap of 0.8 mm. Then, the 3 x 2 mm^2 SWCNT film was deposited. The resistance is extracted in the frequency range 0 -1 GHz. It shows a significant increase from 51.6 to 97.1 Ohms in the presence of NH_3 gas. The electrode with SWCNTS acts as a variable load inserted between the two wings of a bowtie antenna for RFID tag applications. The return loss and radiation pattern are characterized. A return loss higher than 15 dB is preserved at 868 MHz even when the film is bent, illustrating that the device is adequate for applications requiring conformal antennas. The radiation pattern is omnidirectional.

In [70] silver conductive ink is deposited with a FUJIFILM Dimatix DMP-2830 inkjet printer on liquid polyimide supported on a Kapton film. A dual frequency band patch antenna was fabricated to operate at 5 GHz, with dimensions 20.3 mm by 15.6 mm. The measurements show that return loss higher than 20 dB is achieved around 4.9 and 5.6 GHz while omnidirectional radiation is observed at 4.9 GHz.

In [72] a quasi-Yagi planar antenna is proposed. A Dimatix materials printer (DMP-2831) has been used for antenna prototyping, along with graphene ink from Sigma-Aldrich, and a Kapton polyimide film of a height of 125 μm. The overall size is 30 x 20 mm^2. Return loss of 30 dB is obtained at 5.5 GHz, and is preserved when the antenna is bent to a convex or concave shape, as illustrated in Figure 8. Authors conclude that the antenna is suitable” for several wireless applications such as future conformal, flexible and printed electronic devices.”

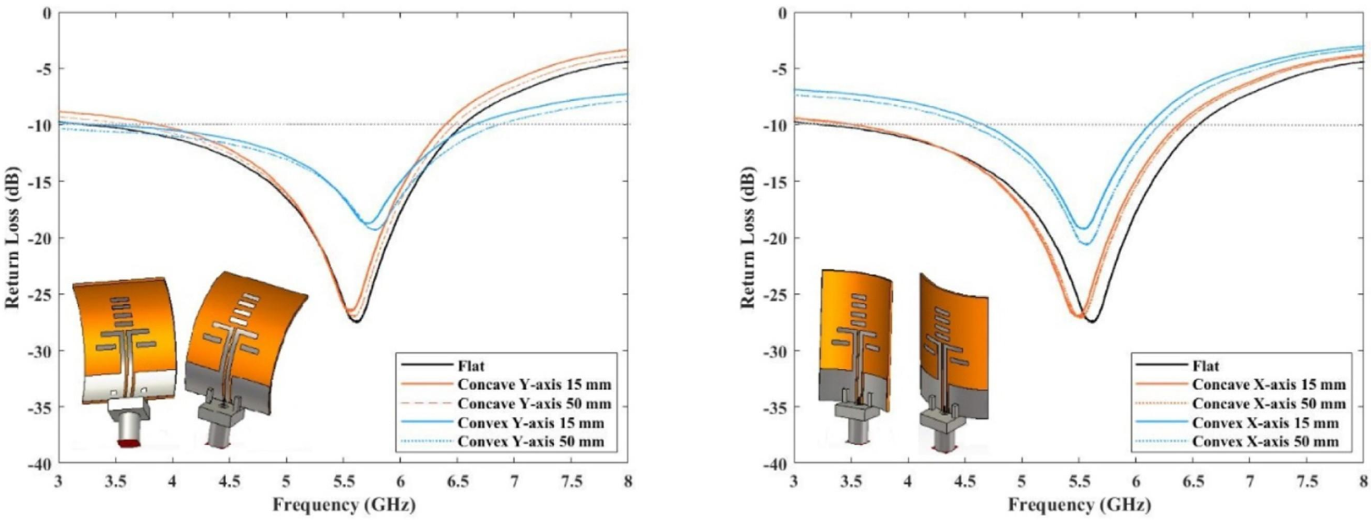

Figure 8. Left: return loss of the Yagi antenna under longitudinal bending. Right: return loss of the Yagi antenna under lateral bending. Reprinted from [72] under the terms of the Creative Commons Attribution 4.0 licence..

Another antenn for gas sensingis proposed in [71]. A microstrip patch antenna is printed on a paper substrate using a DMP-2800 ink-jet printer and silver ink. The feed of the patch is loaded with a parallel stub hosting a CNT film The detection of ammonia is achieved by measuring the shift of the resonant frequency in the presence of ammonia. A shift is observed from 4.7 to 4.5 GHz when ammonia is present. It is explained by the fact that ammonia modifies the resistivity of CNT.

In [73] IJP is considered to realize antennas on textiles for wireless and wear applications. Dimatix DMP-2831 inkjet printer was used in this research with silver ink. Four different substrates are considered: Kapton polyimide film, a stretchable fabric, a polyester fabric, and a polyester/cotton fabric. The printed antenna is a dipole of size 41 x 85.5 mm^2. The measured return loss exceeds 20 dB around 1.9 GHz for polyester and polyester-cotton fabrics.

In [74] a substrate-integrated waveguide (SIW) antenna is printed on a paper substrate using a Dimatix DMP2800 inkjet printer and silver ink. Four slots are inserted in the top metallization of the SIW in order to radiate. The overall size of the antenna is estimated equal to 25 x 150 mm^2. The measured return loss remains higher than 10 dB from 5.2 to 6.4 GHz. The authors conclude that the structure combines the advantages of low-cost, flexible, and environmentally friendly material with the integration potential of SIW technology.

For the sake of completeness, a SIW structure on a paper substrate is also presented in [10]. It operates from 3 to 8 GHz. The structure and its performance are illustrated in Figure 9.

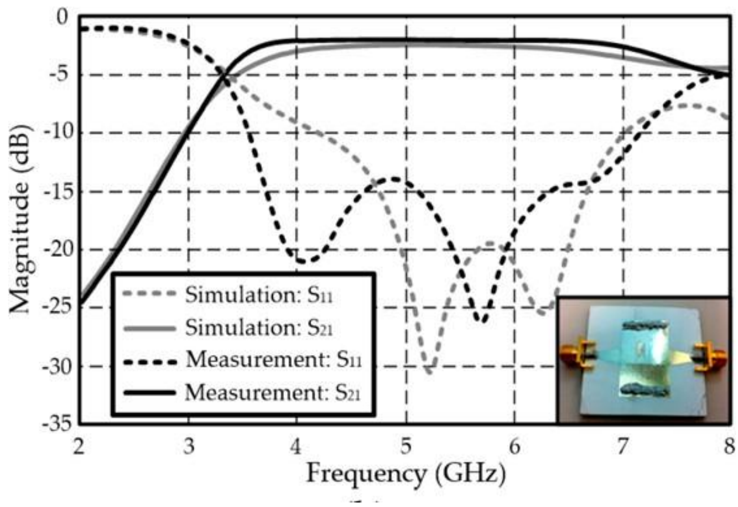

Figure 9. Microstrip-to-SIW transition inkjet printed on a paper substrate using silver ink. The transition consists of two triangular tapered strips connecting the coaxial connectors to the input and output of the rectangular SIW. Reprinted from [10] under CC BY 4.0 license by MDPI.

Chang et al. [75] present a 35.0 × 35.0 × 2.7 mm^3 compact, low-profile, and lightweight wearable antenna for on-body wireless power transfer. The proposed antenna is printed on flexible tattoo paper 5 μm thick using silver epoxy and transformed onto a PDMS substrate to allow flexibility and conformability to the human body. The hexagonal-shaped loop antenna (circumference = 215.50 mm) is isolated from the human skin by an FFS consisting of an array of ring resonators printed on PDMS. Return loss of 18 dB is obtained at 2.45 GHz and remains stable when the structure is bent, confirming its relevance for body-wearing applications.

For the sake of completeness, it is worth mentioning that Orecchini et al. [76] presented an overview of antennas and tags printed on paper substrates realized via IJP for ultra-low-cost radio frequency identification.

3.6. Sensors

As discussed in the previous sections, various topologies of sensors exploit a resonator or an antenna configuration. In this section, we review some additional structures.

In [77] Split Ring Resonators (SRRs) are developed for liquid sensing. The SRR is printed with silver ink on a PMMA substrate of size 76 x 52 mm^2. Microfluidic channels are engraved in a bottom layer to feed the area close to the gaps with the liquid under the scope. The resonant peak observed in the measured reflection loss shifts from 1.6 to 1.458 GHz when glucose is added to deionized water in the microfluidic channel.

In [78] a resonator structure consisting of a parallel network of 50 electrodes is proposed for sensing. The gap between two successive electrodes is equal to 300 μm. The width of the resonator is 14 mm and its main length is 17.2 mm. Microstrip lines are considered as accesses. Dimatix Materials Printer Model DMP-2800 is used with silver ink to print the resonator on an Epson photo paper. The sensitive part of the sensor is printed with PolyInk (PEDOT: PSS-MWCNTs) containing carbon nanotubes (CNTs). The CNT film is expected to be sensitive to vapor of ethanol and toluene. Another resonator having the same dimensions is fabricated without sensitive CNT ink as a reference. The shift of resonant peak decreases with increasing gas concentration, with the gas sensor sensitivity equaling -3.37 kHz/ppm.

In [10] another gas sensor is presented. Its operation is based on the detection of a change of the measured impedance in the presence of NH_3 gas which induces a change of the reflection coefficient of a TAG including an inkjet printed Single Wall CNT film deposited on paper, as illustrated in Figure 10. The presence of the gas modifies the resistivity of the SWCNT film, hence the impedance of the TAG.

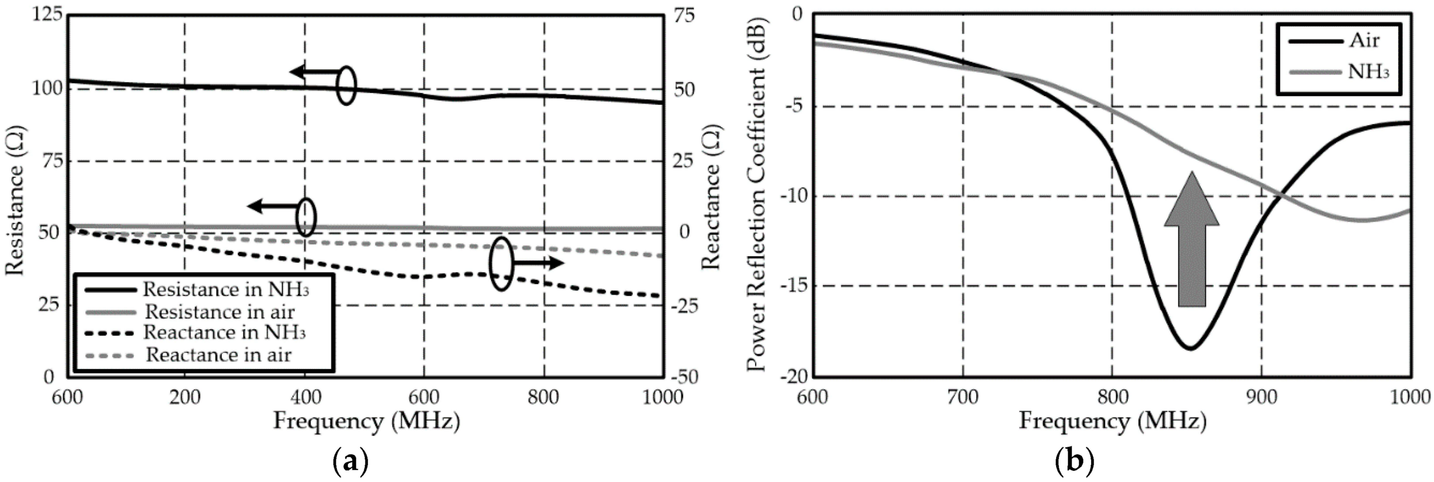

Figure 10. (a) measured impedance of the RFID tag including an inkjet-printed CNT film in the presence of air and NH_3 gas (b) reflection coefficient in the presence of air and NH_3, Reprinted from [10] under CC BY 4.0 license by MDPI.

3.7. Absorbers

Various absorber devices fabricated by IJP have been developed. Most use one or more Frequency Selective Substrate (FFS) structures printed using resistive ink. An array of periodic 2D unit cell patterns usually form an FFS. The array is printed on a substrate traditionally backed by a metallic plane in order to maximize the absorption.

Momeni et al. [38] propose a unit cell consisting of a Swastika cross and an inner resonator ring. A4 copy paper (COPIMAX 80 g/m2) 110 µm-thick was used as the substrate to print the periodic structure using a reactive silver ink. The size of the unit cell is 30.88 mm x 29.915 mm^2. The measured absorption reaches 100% at 6.9 GHz at normal incidence and remains higher than 90% from 6.6 GHz to 7.1 GHz for incidence angles up to 40°.

Another FFS-based absorber is proposed in [79]. The unit cell contains a single 8 branches aster star of diameter 8.019 mm, and the period of the array is equal to 19 mm. 10 x 10 cells of the FFS array are printed on paper with silver ink. The printed FFS is placed on a foam substrate backed by a metallic plate. The measured return loss remains higher than 20 dB between 8 and 15 GHz, with a maximum of 40 dB around 10 GHz.

In [80] a cell formed by 4 concentric hexagonal strips is printed on a 0.14 mm thick substrate using a conductive ink. Reflection loss higher than 10 dB is observed from 9 to 24 GHz.

Yoo et al. [81] propose an FSS unit cell combining a concentric Jerusalem cross and a square ring resonator. The overall size of the unit cell is 5.7 x 5.77 mm^2. The array containing 13 x 13 unit cells is printed on 0.23-mm-thick Kodak premium photo paper using silver ink and a Dimatix DMP2800 inkjet printer. An absorption higher than 90% is preserved around 9.1 GHz for incidence angles ranging from 0 ° to 30°.

Jaiswar et al. [35] propose a similar structure combining Jerusalem crosses and double and single-ring resonators. The structure includes two inkjet-printed FFS layers including 6x6 cells and separated by dielectric spacers 1.5 and 0.75 mm thick, while the top cover layer is 0.25 mm-thick. The total structure is backed by a metallic plate acting as a perfect electric conductor (PEC). The two FFS are printed on 22 μm-thick Lexan films using a Dimatix 2800 material printer and an ink containing carbon nanotubes decorated by magnetic Fe_3O_4 nanoparticles. The overall size of the unit cells is 9 x 9 mm^2, and the thickness of the absorber is 3 mm. The absorber shows absorption superior to 90% over an exceptional 36 GHz bandwidth. The main features of the absorber are summarized in Figure 11. It is worth noticing that the presence of magnetic particles contributes to enhance the absorption. The same structure printed with an ink containing only CNT has a 34% GHz bandwidth of absorption above 90%, as shown in [34].

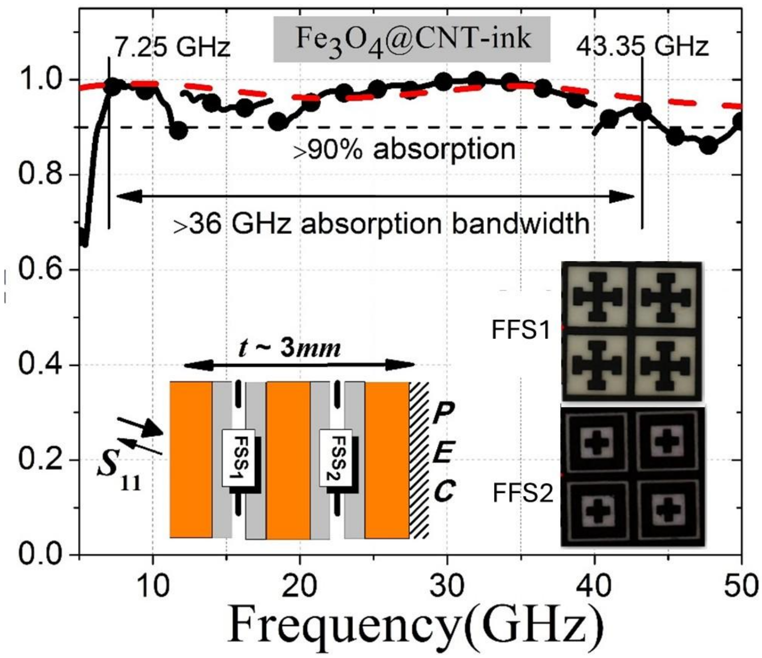

Figure 11. Absorption performance of multilayered structure shown in inset; the photos zoom on a 4x4 array of printed cells for top FFS1 and bottom FFS2, Adapted from [35,82].

In [83] 4 arrays of square grids are printed with silver ink on a flexible paper substrate. The size of the grid/cell is 1 cm, and the array has 21 x 21 cells. The 4 arrays are stacked, so the structure's total thickness equals 1.07 mm. An absorption higher than 90% is preserved from 8.5 to 10.5 GHz, for incidence angles ranging from 0° to 30°.

Machado et al. [84] developed an array of 8 x 15 mm^2 inkjet-printed hexagonal patches arranged in a honeycomb configuration. The array is printed on a PET substrate of thickness 140 µm using silver ink. Return loss above 10 dB is observed between 8 GHz and 11 GHz.

In [85], two concentric square loop resonators are proposed as unit cells of a FFS, with a size of 6.03 x 6.03 mm^2. The array is printed on a 2 mm thick TPU substrate using carbon ink and is backed by an aluminum conductive layer. The overall size of the printed array is 500 x 200 mm^2. A reflectivity lower than -10 dB is obtained from 8.4 to 12.4 GHz.

In [86] the proposed unit cell contains 4 quarter portions of ring resonators (RR) connected by a resistive strip to form a complete RR, printed by inkjet as well as the SRR; the ink for the RR is conductive (silver), while that of the strip is resistive. The lateral size of the unit cell is equal to 14.4 mm. Two arrays of 13 x 13 cells are printed on a Novatek film. Each film is placed on a rubber substrate having 1.5 mm and 2.5 mm thicknesses, respectively. The substrates are stacked together, then the lower one is backed by a metallic layer. The overall thickness of the substrate is 4 mm, while its size is 187.2 x 187.2 mm^2. When adjusting the ratio of surface resistivity of silver and CNT layers to 40/150, a reflectivity inferior to 1% is experimentally observed between 8 and 12 GHz.

3.8. *Origami structures*

For the sake of completeness, it is worth mentioning that IJP has promoted the development of Origami-based flexible electronics. A review of applications is given in [87]. The Origami concept brings 2D IJP to the third dimension by folding inkjet-printed surfaces. The authors illustrate various applications including antennas and sensors. This concept allows to build reconfigurable structures without requiring mechanical supports.

An illustration is provided in [88]. The authors develop inkjet printed antennas with silver ink that are integrated into a flying robot realized using classical origami techniques to fold a photo paper into a bird shape. When the antenna is located on the robot's spine, as illustrated in Figure 12, the authors claim that tuning the angle of the wings does not affect the antenna's radiation pattern, which remains omnidirectional.

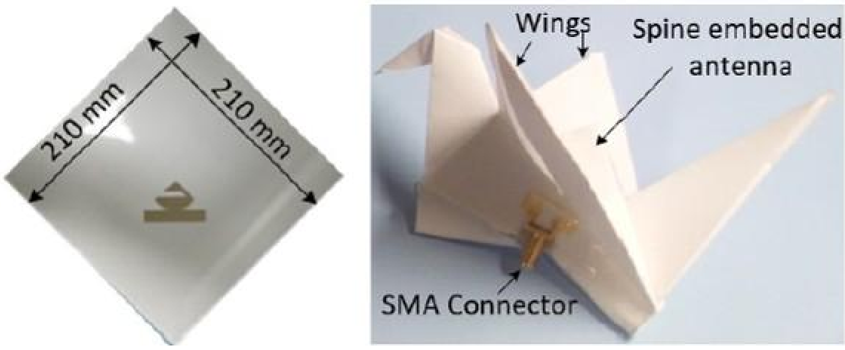

Figure 12. Left: unfolded structure showing at the center the antenna printed on photo paper using silver ink. Right: folded origami bird-like structure, fed by a coaxial connector on the spine. Reproduced from [88] under a Creative Commons Attribution 4.0 License by IEEE. For more information, see https://creativecommons.org/licenses/by/4.0/I.

Shen et al. [89] applied the Origami concept to absorbers. An array of 16 x 16 folded resistive patches is printed on a flexible PET substrate 0.1 mm thick. The size of the unit cell is 31.7 x 31.7 mm^2. The authors claim that their structure minimizes the reflectivity and thus maximizes the absorption from 0° to 75° incidence angle between 3 and 13 GHz.

Another origami-based absorber is presented in [90]. A Tachi–Miura origami pattern arranged in a honeycomb configuration is proposed to create an absorber using carbon-based ink deposited on cardstock paper. The measured reflectivity remains below 10 dB in the frequency range from 0 to 30 GHz, ensuring more than 90% absorption, as shown in Figure 13. Authors claim that this performance is preserved from 0° to 70° incidence angle.

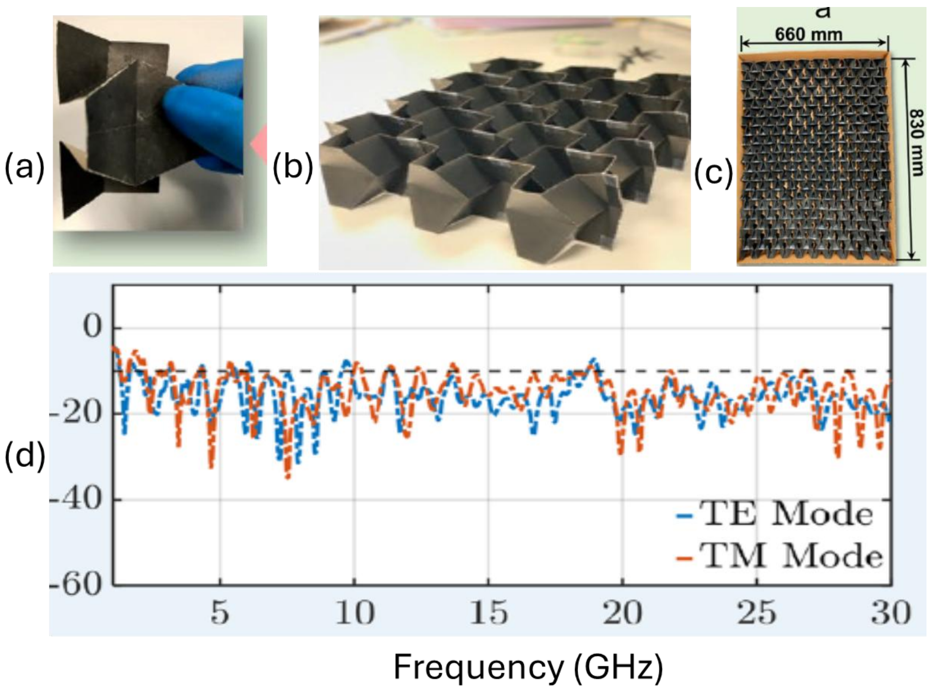

Figure 13. Origami-based absorber structure (a) hand-folding of the structure (b) perspective view of the folded structure (c) top view of the absorber prototype (d) reflectivity measurement. Reproduced and adapted from [90] under a Creative Commons Attribution 4.0 International License by Springer. For more information, see https://creativecommons.org/licenses/by/4.0.

Zhu et al. [91] propose an array of rooftop-folded strips printed on a polyimide film supported by a Teflon substrate, arranged in a honeycomb configuration. The measured reflectivity remains below 20 dB from 3 to 20 GHz whatever the incidence angle comprised between 0° and 70°.

4. Conclusive discussion

In this review, the fabrication and performance of microwave inkjet-printed passive microwave devices have been discussed. The result of their analysis is summarized in Tables 1 and 2. Couplers, resonators, sensors, absorbers, and antennas are presented. According to the various works cited, IJP has been used for this purpose since 2010 and new developments are still being proposed in the 2020', including green substrates and inks, as well as sensors and absorbers. IJP on paper is often promoted owing to its obvious sustainability and low-cost advantages. Origami-based structures offer the additional advantage of facile reconfigurability for antenna applications without a need for mechanical support.

Tables 1 and 2 show that inks based on silver are mostly used for IJP, followed by carbon-based materials. The most developed devices are antennas and absorbers for wireless communications and on-body applications, and radar and electromagnetic compatibiltity situations, respectively.

According to the state-of-the-art proposed in this review, realizations based on IJP seem limited to the microwave frequency range for the moment. Monitoring the literature in the coming years would be relevant to update this review towards the millimeter-wave range.

Funding: This work was supported by the National Fund for Scientific Research, FNRS, Belgium, were I.H. is appointed as Research Director. The APC was funded by UCLouvain.

Data Availability Statement: No new data were created in this study.

Conflicts of Interest: "The authors declare no conflicts of interest." .

Abbreviations

The following abbreviations are used in this manuscript:

BCB	Benzo-cyclo-butene
BST	Barium Strontium Titanate
CNT	carbon nanotube
DC	direct current
FSS	frequency selective surface
IDC	interdigitated capacitor
IJP	inkjet printing
IoT	Internet of Thinks
LCP	liquid crystal polymer
LTCC	low temperature cofired ceramic
MEMS	micro electromechanical system
MIM	metal-insulator-metal
PBS	polybutylène succinate
PCL	polycaprolactone
PDMS	polydimethylsulfide
PE	polyethylene
PEG	polyethylene glycol
PGLA	polyglycolic acid
PLA	polylactic acid
PI	polyimide
PTFE	polyethylene terephtalate
PU	polyurethane
PVP	polyvinyl phenol
PVDF	poly(vinylidene fluoride)
RF	radio frequency
RFID	radio frequency identification
SIW	substrate integrated waveguide
SU-8	name of an epoxy-based negative photoresin
SRR	split ring resonator
SWCNT	single wall carbon nanotube
TPU	thermoplastic polyurethane
UV	ultra-viol

Table 1. Summary - Part I.

Device type	Ink type	substrate	Topology	Operational frequency	Applications	Ref.
Couplers	silver	Rogers 4003C	3 dB interdigitated Lange-type	8	antenna systems	[5]
	silver	PI	broadband 3 dB SIW	5	sensing	[6]
	silver	PET	3 dB branchline	5.09 - 6.97	phased array & beamforming	[63]
Capacitors	silver	PI	IDC	1 - 5	MIC	[2]
	Voltera Flexible Conductor 2	SU - 8 and PVP	MIM	1.9 - 3	wearable systems	[64]
Resonators	silver	LTCC	microstrip ring	2.5 - 3.2	microfluidic sensing	[65]
	gold	PI	microstrip SRR	2.65	sensing	[66,67]
	CNT ink	Rogers Laminate	square resonator	3 - 7	NH_3 sensor	[52]
	silver	SU - 8	T-resonator	2.2 - 30	dielectrometer	[69]
Filters	silver	low-cost FR4	low-pass & bandpass microstrip filter	0 - 8	planar microwave circuits (MC)	[4]
Antennas	silver	low-cost FR4	stepped monopole	1 - 12	planar MC	[4]
	silver	Rogers RO 3203	microstrip patch	2.4	wireless coms	[9]
	silver	paper	microstrip Z-shaped monopole	0.9	RFID	[50]
	silver	PI	bowtie config.	4.91	gas detection	[51]
	graphene ink	PI	planar Yagi	0.9	on body wireless coms	[72]
	silver	paper	microstrip patch including a sensitive CNT film	4.5	NH_3 sensor	[71]
	silver	polyester fabric	microstrip dipole	1.9	wireless on-body apps	[73]
	silver	paper	slotted SIW	5.2 - 6.4	wireless coms	,[74]
	Ag-In-Ga liquid metal alloy	Tatoo paper/PDMS	hexagonal loop + ring FFS	2.4	on body wireless power transfer	[75]
Sensors	silver	PMMA	SRR	2.45	Microfluidic glucose detection	,[77]
	PolyInk (PEDOT: PSS-MWCNTs)	Epson photo paper	parallel network of 50 strip electrodes	3	detection of ethanol & toluene	[78]
			RFID tag			

	-	paper	including a sensitive CNT film	0.860	Detection of ammonia NH_3	[10]

Table 2. Summary - Part II.

Device type	Ink type	substrate	Topology	Operational frequency	Applications	Ref.
FSS-absorbers	reactive silver	A4 copy paper	Swastika cross + inner ring	6.6 - 7.1	wireless coms	[38]
	silver	paper	8 branch aster star	8 – 15	na	[79]
	graphite-based	Taconic TLY-5	4 concentric hexagonal strips	9 - 24	On-body sensors	[80]
	silver	Kodak photo paper	Jerusalem cross + square ring	9.1	Conformable scenarii	[81]
	CNT decorated wirh Fe_3O_4 nanoink	Lexan PI	Jerusalem cross + double an single SRRs	7.25 – 43.35	Radar	[35]
	silver	paper	array of square grid	8.5 – 10.5	electromagnetic compatibility	[83]
	silver	PET	Hexagonal patches	8 – 11	satellite & other aerodynamic configs	[84]
	CNT- based	TPU	concentric square loop resonators	8.4 -12.4	stealth & electromagnetic compatibility	[85]
	silver	Novatek film	array of ring resonators	8 - 12	radar & mobile coms	[86]
Origami structures	silver	paper	antenna printed on bird-shaped origami	2.4 – 5.2	flying robots	[88]
	carbon - based	flexible PET	array of 16 x 16 folded resistive patches	3 - 13 GHz	stealth technologies & electromagnetic interference	[89]
	carbon - based	Cardstock paper	Tachi–Miura origami pattern arranged in a honeycomb configuration	0 - 30	mitigate signal interference & shield electromagnetic systems	[90]
	MWCNT + COOH	PI	array of rooftop-folded strips arranged in honeycomb configuration	na	PV flexible electronics	[91]

References

1. El Hajjaji C; Delhote N; Verdeyme S; Piechowiak. Optimization of the conductivity of microwave components printed by inkjet and aerosol jet on polymeric substrates by IPL and laser sintering. *International Journal of Microwave and Wireless Technologies* **2021**, *13*, 652 – 662.
2. Gugliandolo G; Alimenti A; Torokhtii K; Pompeo N; Campobello G; Crupi G; Silva E; Donato N. Design and test of an inkjet-printed microwave interdigital capacitor on flexible Kapton substrate. In Proceedings of 23rd International Wor kshop on ADC and DAC Modelling and Testing IMEKO TC-4 2022, Brescia, Italy / September 12-14, 2022, 346 - 351
3. McKerricher G; Vaseem M; Shamim A. Fully inkjet-printed microwave passive electronics. *Microsystems & Nanoengineering* **2017**, *3*, 16075.
4. Blanco-Angulo C.; Martinez-Lozano A; Arias-Rodriguez J.; Rodriguez-Martinez A; Vincente-Samper JM; Sabater-Navaro JM; Avila-Navar E. Low-Cost Direct-Writing of Silver-Based Ink for Planar Microwave Circuits up to 10 GHz. *IEEE Access* **2023**, *11*, 4010 – 4022.
5. He X; Tentzeris MM. Inkjet Printed Lange Coupler for Antenna Systems. In Proceedings of 2019 IEEE International Symposium on Antennas and Propagation and USNC-URSI Radio Science Meeting 2019, Atlanta, GA, USA / 07-12 July 2019, 91 - 92.
6. Kim S; Aubert H; Tentzeris M. An Inkjet-printed Flexible Broadband Coupler in Substrate Integrated Waveguide (SIW) Technology for Sensing, RFID and Communication Applications. In Proceedings of the 2014 IEEE MTT-S International Microwave Symposium (IMS2014), Tampa USA, 01-06 June 2014, 4 p:
7. Godlinski D; Zichner R; Zöllmer V; Baumann RR. Printing technologies for the manufacturing of passive microwave components: antennas *IET Microw. Antennas Propag.* **2017**, *11*, 2010 - 2015.
8. Kim S; Cook B; Le T; Cooper J; Lee H; Lakafosis V; Vyas R; Moro R; Bozzi M; Georgiadis A; Collado A; Tentzeris MM. Inkjet-printed antennas, sensors and circuits on paper substrate *IET Microw. Antennas Propag.* **2013**, *7*, 858 – 868.
9. Al-Naiemy Y; Elwi TA; Khaleel HR; Al-Rizzo H. A Systematic Approach for the Design, Fabrication, and Testing of Microstrip Antennas Using Inkjet Printing Technology. *International Scholarly Research Network* **2023**, *2012*, 132465.1-11.
10. Kim S. Inkjet-Printed Electronics on Paper for RF Identification (RFID) and Sensing *ISensors* **2020**, *9*, 1636.1-22. L
11. Azucena O; JKubbyJ; Scarbrough D; Goldsmith C. Inkjet Printing of Passive Microwave Circuitry. In Proceedings of the 2008 IEEE MTT-S International Microwave Symposium Atlanta, GA, USA / 15-20 June 2008, 1076 - 1078.
12. Rosker ES; Sandhu R; Hester J; Goorsky M.S; Tice J. Printable Materials for the Realization of High Performance RF Components: Challenges and Opportunities *IInternational Journal of Antennas and Propagation* **2018**, *2018*, 19 p.
13. Friederich F; Kohler C; SazegarM; Nikfalazar M; Jakoby R; Binder J.R; Bauer W. In Proceedings of the IMAPS/ACerS 9th CICMT Conference (2013) Orlando, Florida USA/ April 23-25 , 2013, 000232 - 000239.
14. Zhang H ; Lan Y; Qiu S; .Min S, Jang H, Jeongpil Park J; Song S; Ma Z. Flexible and Stretchable Microwave Electronics: Past, Present, and Future Perspective. *Adv. Mater. Technol.* **2021**, *6*, 2000759
15. Singh M, Hanna M. Haverinen HM, Dhagat P, E. Jabbour GE. Inkjet Printing—Process and Its Applications. *Adv. Mater.* **2010**, *22*, 673–685.
16. Mack Grubb P, Subbaraman P.A.; Park S.; Akinwande D.; Chen R.T. Inkjet Printing of High Performance Transistors with Micron Order Chemically Set Gaps. *Scientific Reports* **2017**, *7*, 1202.1- 7.
17. Kamyshny A.; Steinke J. ;Magdassi S. Metal-based Inkjet Inks for Printed Electronics *The Open Applied Physics Journal* **2011**, *4*, 19-36.
18. Nabatian D.J.; Rosenwald C.; F. Barlow F.; Kabir H. A Study of Microwave Behavior of a Thin-Print Gold Ink. In Proceedings of the 2002 International Symposium on Microelectronics: September 4-6, 2002, Colorado Convention Center, Denver, USA.
19. Ohlund T.; Schuppert A.; Andres B.; Andersson H.; Forsberg S.; Schmidt W.; Hans-Erik Nilsson,H.E.: Andersson M.; Renyun Zhanga R.; Olina H. Assisted sintering of silver nanoparticle inkjet ink on paper with active coatings *RSC Adv.* **2015**, *5*, 64841.1 - 9.
20. Li R-Z.; Hu A.; Bridges D.; Zhang T.; Oakes K.D.; Peng R.; Uma Tumuluri U.; Wue Z.; Feng Z. Robust Ag nanoplate ink for flexible electronics packaging *Nanoscale* **2015**, *7*, 7368-7377.
21. Khondoker M.A.H.; Mun S.C.; Kim J. Synthesis and characterization of conductive silver ink for electrode printing on cellulose film *Applied Physics A.* **2013**, *112*, 411 - 418.
22. Rao V.K. Abhinav K V.,. Karthik P; Prakash Singh S. Conductive silver inks and their applications in printed and flexible electronics *RSC Adv.* **2015**, *5*, 77760. - 77790.
23. Li R.Z.; Hu A.; Zhang T.; Oakes K.D.; Direct Writing on Paper of Foldable Capacitive Touch Pads with Silver Nanowire Inks *Appl. Mater. Interfaces* **2014**, *6*, 21721 – 21729.
24. Bjorninen T.; Merilampi S.; Ukkonen L.; Ruuskanen P. s L. Sydanheimo L.;. Performance comparison of silver ink and copper conductors for microwave applications *IET Microw. Antennas Propag.* **2010**, *4*, 1224–1231.
25. Abhinav K V.; Rao V.K.; P. S. Karthika P.S.; Prakash Singh S. Copper conductive inks: synthesis and utilization in flexible electronics *RSC Adv.* **2015**, *5*, 63985 - 64030.
26. Tortorich B.P.; Choi J-W. Inkjet Printing of Carbon Nanotubes *Nanomaterials* **2013**, *3*, 453 - 468.
27. Wei T.; Ruan J.; Fan Z.; Luo G.; Wei F. Preparation of a carbon nanotube film by ink-jet printing *Carbon* **2007**, *45*, 2692 – 2716.
28. Loffredo F.; , De Girolamo Del Mauroa A.; Burrasca G.; V. La Ferrara V.; Quercia L. Ink-jet printing technique in polymer/carbon black sensing device fabrication *Sensors and Actuators B* **2009**, *143*, 421 – 429.
29. Huang X.; Leng T.; Chang K.H.; Chen J.C.; Novoselov K.S.; Hu Z. *2D Mater.* **2007**, *3* 025021.

30. Giardi R.; Porro S.; Chiolerio A.; Celasco E.; Sangermano M. Inkjet printed acrylic formulations based on UV-reduced graphene oxide nanocomposites *Carbon* **J Mater Sci**, **2013**, *48*, 1249–1255.
31. Torrisi F. et al. Inkjet-Printed Graphene Electronics. *ACS Nano* **2007**, *6* 2992–3006.
32. Secor E.B.; Prabhumirashi P.L.; Puntambekar K.; Geier M.L.; Hersan M.C. Inkjet Printing of High Conductivity, Flexible Graphene Patterns. *J. Phys. Chem. Lett.* **2013** *4* 1347
33. Perelaer J.; Smith P.J.; Mager D.; Soltman D.; Volkman S.K.; Subramanian V.; Korvinkdf J.G.; Schubert U.S. Printed electronics: the challenges involved in printing devices, interconnects, and contacts based on inorganic materials. *J. Mater. Chem.* **2010**, *20* 8446–8453.
34. Jaiswar R.; · F. Mederos-Henry F.; Hermans S.; Raskin J.P.; Huynen I. Inkjet-printed Frequency Selective Surfaces based on carbon nanotubes for ultra-wideband thin microwave absorbers. *J Mater Sci: Mater Electron* **2020**, *31* 2190–2201.
35. Jaiswar R.; · F. Mederos-Henry F.; Dupont V.; · Hermans S.; Raskin J.P.; Huynen I. A ultra-wideband thin microwave absorber using inkjet-printed frequency-selective surfaces combining carbon nanotubes and magnetic nanoparticles. *Applied Physics A* **2019**, *479*) 125 : 473.
36. Oueriemi I.; Raskin J.P.; Choubani F.; HuynenI. Wideband non-linear characteristics of random multi-walled carbon nanotube networks. *Microwave and Optical Technology Letters* **2013**, *55* 2648 – 2652.
37. De Paolis R.; Pacchini S.; Coccetti F.; Monti G.; Tarricone L.; Tentzeris M.M.; Plana R. Circuit Model of Carbon-Nanotube Inks for Microelectronic and Microwave Tunable Devices. In Proceedings of the 2011 IEEE MTT-S International Microwave Symposium Baltimore, USA 05-10 June 2011
38. Momeni-Nasab M.:, Bidoki S.M.; Hadizadeh M. Ink-jet printed metamaterial microwave absorber using reactive inks. *Int. J. Electron. Commun.* **2020**, *123* 153259.1 - 9
39. Smith P.J.; Morrin A. Reactive inkjet printing. *J. Mater. Chem.* **2012**, *22* 10965 - 10970.
40. Kheawhom S.; Foithong K. Comparison of Reactive Inkjet Printing and Reactive Sintering to Fabricate Metal Conductive Patterns. *Japanese Journal of Applied Physics* **2013**, *52* 05DB14.
41. Kim H. et al. Barium titanate-enhanced hexagonal boron nitride inks for printable high-performance dielectrics. *Nanotechnology* **2022**, *32* 2157042.1 - 8.
42. Mohapatra A.; Tuli S.K.; , K-Y.; Tomoko Fujiwara T.; Hewitt Jr R.W.; Frank Andrasik F.; Morshed B. Inkjet Printed Parallel Plate Capacitors Using PVP Polymer Dielectric Ink on Flexible Polyimide Substrates. In Proceedings of the 2018 40th Annual International Conference of the IEEE Engineering in Medicine and Biology Society (EMBC) Hawaii Honolulu USA/ 18-21 July 2018, 000232 - 000239.
43. Piro Y.; Areias, C.; Luce A.; Michael M.; Biswas P.; Ranasingha O.; Reuther J.F.; Trulli S.; Akyurtlu A. Low-Loss Dielectric Ink for Printed Radio Frequency and Microwave Devices. *CS Appl. Mater. Interfaces* **2023**, *15*
44. Goulas A.: et al. Direct ink writing of bismuth molybdate microwave dielectric ceramics. *Ceramics International* **2021**, *47*) 7625 – 7631.
45. Haghzadeh M.; Armiento C.; Akyurtlu A. Fully Printed Varactors and Phase Shifters Based on a BST/Polymer Ink for Tunable Microwave Applications. In Proceedings of the 2016 IEEE MTT-S International Microwave Symposium (IMS) San Francisco, USA/ 22 - 27 May 2016.
46. Eshkeiti M.; et al. Screen Printing of Multilayered Hybrid Printed Circuit Boards on Different Substrates. *IEEE Trans. Components, Packaging and Manufacturing Techn.* **2015**, *5*) 415 - 421.
47. Ali Shah M.; Lee D.G.; Lee B-Y.; Hur S. Classifications and Applications of Inkjet Printing Technology: A Review. *IEEE Access* **2021**, *9* 140077 – 140102.
48. Serpelloni M.; Cantù E.:, Michela Borghetti M.; Sardini E. Printed Smart Devices on Cellulose-Based Materials by means of Aerosol-Jet Printing and Photonic Curing. *Sensorsl* **2020**, *20* 841.1-18.
49. Lessing J.; , Ana C. Glavan A.C.; , S. Brett Walker B.:, Christoph Keplinger C.; Lewis J.A.; Whitesides G.M. Inkjet Printing of Conductive Inks with High Lateral Resolution on Omniphobic “R F Paper” for Paper-Based Electronics and MEMS. *Advanced Mater.* **2014**, *26* 4677–4682
50. Konstas Z.; Rida A.; Vyas R.; Katsibas K.; Uzunoglu N.;Tentzeris M.M. A Novel “Green” Inkjet-Printed Z-Shaped Monopole Antenna for RFID Applications. In Proceedings of the 2009 3rd European Conference on Antennas and Propagation, Berlin, Germany/ 23-27 March 2009.
51. L.i Y.; Zhang R.; Staiculescu D.; Wong C.P.; Tentzeris M.M. A Novel Conformal RFID-Enabled Module Utilizing Inkjet-Printed Antennas and Carbon Nanotubes for Gas-Detection Applications. *IEEE Ant. Wireless Propag. Lett.* **2009**, *8* 651 - 653.
52. Kao H-L.;, Tsai Y-C.: Chang L.C.; Chiu H.C. Microwave Resonators Embedded With Carbon Nanotubes for Real-Time Gas Sensing. *IEEE Sensors Journall* **2024**, *24* 4325-4334.
53. Sanchez-Duenas L. et al. A Review on Sustainable Inks for Printed Electronics: Materials for Conductive, Dielectric and Piezoelectric Sustainable Inks.*Materials* **2023**, *16* 22 p.
54. Hwang Y. et al. Plant-Based Substrate Materials for Flexible Green Electronics. *Advanced Mater. Technology* **2022**, *7* 2200446.1 - 10.
55. Scandurra G.; Arena A.; Ciofi C. A Brief Review on Flexible Electronics for IoT: Solutions for Sustainability and New Perspectives for Designers. *Sensors* **2023**, *23* 5264.1-31.
56. Jürgensen N.; Pietsch M.; Hai X.; Schlisske S.; Hernandez-G. Green ink formulation for inkjet printed transparent electrodes in OLEDs on biodegradable substrates. *Synthetic Metals* **2021**, *202* 116930.1 - 7.

57. Batet D.; VilasecaF.; Ramon E.; Esquivel J.P.; Gabriel G. Experimental overview for green printed electronics: inks, substrates, and printing techniques. *Flex. Print. Electron.* **2023**, *8* 024001.1-19.
58. Al Shboul A..; Ketabi M.; Izquierdo R. Conductive Green Graphene inks for Printed Electronics. In Proceedings of the 2021 IEEE 16th Nanotechnology Materials and Devices Conference (NMDC), Anchorage, USA/ 12-1R December 2021.
59. Franco M. et al. Environmentally Friendly Conductive Screen-Printable Inks Based on N-Doped Graphene and Polyvinylpyrrolidone. *Adv. Eng. Mater.* **2021**, 2101258.1-11.
60. Hussein R.N.; Schlingman K.; Noade C.; Carmichael S.; Carmichael TB. Shellac-paper composite as a green substrate for printed electronics. *Flex. Print. Electron.* **2022**, *7* 045007.1-13.
61. Li Y.; Misra M.; Gregori S. Printing Green Nanomaterials for Organic Electronics. *IEEE Trans. Comp. Packaging and Manufacturing Tech.* **2018**, *8* 1307 - 1316.
62. Wiklund J.; Karakoç A.;i Palko T.; Yi gitler H.; Ruttik K.; Riku Jäntti R.; Paltakari J. A Review on Printed Electronics: Fabrication Methods, Inks, Substrates, Applications and Environmental Impacts. *Journal of Manufacturing and Materials Processing* **2021**, *5* 36 p.
63. Babale S.A.; Rahim S.K.A.; Himdi M.; Lawan S.H.; F. D. Sani, F.D.; Usman A.D. Implementation of inkjet-printed 3 dB coupler with equal power division and 45 degrees output phase difference. *Microwave and Optical Technology Letters* **2021**, *63* .1007 - 1011.
64. Cook B.S.; Cooper J.R.; Tentzeris M.M. Multi-Layer RF Capacitors on Flexible Substrates Utilizing Inkjet Printed Dielectric Polymers. *IEEE Microw. Wireless Comp. Lett.* **2013**, *23* 353-355.
65. Jasinska L..; SzostakK.; Kiliszkiewicz M.; Słobodzian P.; Malecha K. Ink-jet printed ring resonator with integrated microfluidic components. *Circuit World* **2020**, *46* .301 – 306.
66. Paul M.; Kühnel H.; Oberpertinger R.; Mehofer C.; Pollhammer D.; Wellenzohn M. Two-Layer Inkjet-Printed Microwave Split-Ring Resonators for Detecting Analyte Binding to the Gold Surface. *Sensors* **2024**, *24* 1688.1-13.
67. Paul M.; Kühnel H.; Oberpertinger R.; Mehofer C.; Wellenzohn M. Inkjet-printed Split Ring Resonators for Microwave Sensor Applications on Flexible Kapton Substrate. In Proceedings of the 2023 PhotonIcs & Electromagnetics Research Symposium (PIERS), Prague, Czech Republic,/ 2 - 6 July 2023.
68. Royo I.. , Fernández-García R.; Gil I. Microwave Resonators for Wearable Sensors Design: A Systematic Review. *Sensors* **2023**, *23* 9103.1 - 43.
69. Tehrani B.K.; Bito J.; Cook B.S.; Tentzeris M.M. Fully inkjet-printed multilayer microstrip and T-resonator structures for the RF characterization of printable materials and interconnects. In Proceedings of the 2014 IEEE MTT-S International Microwave Symposium (IMS2014), Tampa FL, USA/ 1-6 July 2014.
70. Kirschenmann K.; Whites K.W.; Woessner S.M. Inkjet printed microwave frequency multilayer antennas. In Ptoceedings of the 2007 IEEE Antennas and Propagation Society International Symposium. Honolulu, USA/ 9 - 15 June 2007.
71. Lee H.; Shaker G.; Naishadham K.; Song X.; McKinley M.; Wagner B.; Tentzeris M. Carbon-Nanotube Loaded Antenna-Based Ammonia Gas Sensor. *IEEE Trans. Microwave Theory Tech.* **2021**, *59* 2665 - 2674.
72. Ibanez Labiano I.; Alomainy A.A. Flexible inkjet-printed graphene antenna on Kapton. *Flex. Print. Electron.* **2021**, *6* 025010.1- 8.
73. Chauraya A.; Whittow W.G.; Vardaxoglou Y.C.; Li Y.; Torah R.; Yang K; Beeby S.; Tudor J. Inkjet Printed Dipole Antennas on Textiles for Wearable Communications *IET Microwaves, Antennas Propagation* **2021**, *7* 760 – 767.
74. Moro R.; Kim S.; Bozzi M.; Tentzeris M. Inkjet-printed paper-based substrate-integrated waveguide (SIW) components and antennas. *IET Microwaves, Antennas and Propagation* **2021**, *7* 760 – 767.
75. Chang X.L.;, Song Chee P.; Lim E.H. Compact conformal tattoo-polymer antenna for on-body wireless power transfer. *Scientific Reports* **2023**, *13* 9678.
76. Orecchini G. Alimenti F.; Palazzari V.. A. Rida A.;Tentzeris M.M.; Roselli L. *IET Microwaves, Antennas and Propagation* **2011**, *5* 993 – 1001
77. Camli B. et al. Rapid prototyping of noncontact microwave microfluidic devices for sensing applications. *J. Micromech. Microeng* **2021**, *31* 097001.1- 8.
78. Georges J. et al. CNT-Based Inkjet-Printed RF Gas Sensor: Modification of Substrate Properties during the Fabrication Process. *Sensors* **2019**, *31* 1768.1- 13.
79. Tirkey M.M; Gupta N. Inkjet-printed broadband FSS-based absorber with improved absorption characteristics. *International Journal of Microwave and Wireless Technologies* **2023**, 1- 9.
80. Zabri Z.N.; Cahill R.; Conway G.; McGuigan N.; Zelenchuk D. ; Dickie R. Manufacturable Ultra-Thin Resistive FSS for Challenging EM Mobile Environments. In 2007 Proceedings of the 12th European Conference on Antennas and Propagation (EuCAP 2018). London, UK/ 9- 13 April 2018.
81. Yoo M.; Kim H.K.: Kim S.; Tentzeris M.; Lim S. Silver Nanoparticle-Based Inkjet-Printed Metamaterial Absorber on Flexible Paper. *IEEE Ant. Wireless Propag. Lett.* **2013**, *14* 1718 - 1722.
82. Jaiswar R. Wideband microwave absorber structures based on carbonaceous nanomaterials: From modelling to experimental Characterisation. PhD Thesis, Université catholique de Louvain, Louvain-la-Neuve, Belgium, 23 April 2019.
83. Tirkey M.M; Gupta N. Broadband Polarization-Insensitive Inkjet-Printed Conformal Metamaterial Absorber. *IEEE Trans. Electromagn. Compat.* **2021**, *63* 1829 - 1837.
84. Machado G.G.; Cahill R.; Fusco V.; Conway G. Design and fabrication of inkjet printed ultrathin FSS based microwave absorbers. In Proceedings of the Loughborough Antennas and Propagation Conference (LAPC 2018). Loughborough, UK/ 12 - 13 November 2018.

85. Han J.S. et al. 29760. Ultrawide meta-film replication process for the mass production of a flexible microwave absorbingmeta-surface. *Optics Express* **2022**, *30* 29761.1 - 12.
86. Han W.; Q-Han Park Q.A.Broadband absorber with dispersive metamaterials. *Nanophotonics* **2023**, *12* 2443–2449.
87. Hester J.G. et. al. Inkjet printing and additive manufacturing technologies (AMT) are introduced for the fabrication of flexible RF/microwave electronics and sensors.. *Proceedings of the IEEE* **2015**, *103* 584–606.
88. Njogu P.M.; Sanz-Izquerdo B.; Jun S.Y; Kalman G.; Gao S.; Malas A.; Gibbons G.J. Evaluation of Planar Inkjet-Printed Antennas on a Low-Cost Origami Flapping Robot. *IEEE Access* **2020**, *8* 164103 - 16425.
89. Shen Y.; Pang Y.; Wang J.; Ma H.; Pei Z.; Qu S. Origami-inspired metamaterial absorbers for improving the larger-incident angle absorption. *J. Phys. D: Appl. Phys.* **2015**, *48*) 445008.1 - 7.
90. Biswas A.; Zekios C.L.; Ynchausti C.; Howell L.L.; Magleby S.P.; Georgakopoulos S.V. An ultra-wideband origami microwave absorber. *Scientific Reports* **2022**, *12* 13449.1 - 16.
91. Zhu Z.; Yongfeng Y.; Qin Z.; Jiang, L.; Wang W.; Chen H.; Wang J.; Zhen L.; Qu S. Miura-ori based reconfigurable multilayer absorber for high-efficiency wide-angle absorption. *Optics Express* **2024**, *32* 24092.1 - 16.